Aust. J. Phys., 1989, **42**, 451–64

Ionospheric E_s in the Southern Hemisphere Temperate Zone. I. Seasonal Characteristics of $f_0 E_s$

W. J. Baggaley

Physics Department, University of Canterbury,
Christchurch 1, New Zealand.

Abstract

Detailed seasonal variations of $f_0 E_s$ occurrence are presented for the Southern Hemisphere Temperate zone from the analysis of approximately twenty years of ionosonde data for ten stations (9°·4 to 52°·6 geographic latitude) in the Australasian region. Significant short term features are found: a late autumn enhancement strongest at about 20°S and evidence of a secondary summertime peak one month before the solstice. A comparison between the gross seasonal characteristics of $f_0 E_s$ occurrence with those expected from a simple model of the wind shear mechanism shows similar latitude trends, though the model predicts autumn equinox values which are too low.

1. Introduction

The ionospheric *E*-region (100–130 km) often contains ionisation irregularities which occur both in space and time in a quasi-random fashion. The term sporadic-*E* has long been used to describe this genre: it is not clear if the term really applies to several aeronomically separate species. Sporadic-*E* is known to have different properties according to geographical/geomagnetic location; the equatorial, temperate and auroral types. The demarcations probably correspond to distinct mechanisms involved in E_s formation.

Several techniques have been employed in the study of E_s ionisation characteristics: rockets, swept-azimuth fixed frequency sounders recording E_s-propagated ground-scatter, oblique HF communication links, ionosondes and incoherent scatter radars. Each technique may investigate different aspects of the ionisation irregularities so intercomparisons may not necessarily relate to the same aeronomical properties.

Routine ionosonde programmes have been maintained on a global scale for some decades and such surveys permit regular sampling (at hourly intervals for most published data) of the E_s region. The parameters of interest scaled from ionograms are: $f_0 E_s$—the highest frequency for which a continuous reflection is present for ordinary ray propagation; $f_b E_s$ (blanketing frequency)—the lowest ordinary wave frequency at which the E_s layer becomes transparent; and $h'E_s$—the virtual height of the reflection. Most models identify $f_0 E_s$ with the maximum plasma frequency within a Fresnel zone and $f_b E_s$ with the mean plasma frequency of the layer. International scaling rules allow data

0004-9506/89/040451$03.00

from different stations and scaled by different personnel to be compared with confidence. Interpretation of ionogram traces may be complicated by several factors such as oblique echoes or mode coupling.

Patches of E_s ionisation are localised in space (typically scale sizes of a few hundred kilometres horizontally and of the order of 1 km vertically) and time (duration a few hours) and occur spatially and temporarily in an irregular quasi-random fashion. Clearly, hourly sampling of such a phenomenon will yield rather limited information for individual E_s patches (compared with, for example, rocket sampling) but the morphological data resulting from regular synoptic surveys are valuable in attempting to isolate the factors governing E_s formation maintenance and decay. Smith (1978) gave maps depicting the broad features of the geographical distribution and limited seasonal variation. Because of large year to year variability in E_s occurrence, the accumulation of several years of data is necessary to obviate the effects of large statistical fluctuations. The task of such studies is to isolate the various functions necessary for E_s and to relate these functions to models of E_s production.

There is much evidence (Whitehead 1970) to support the wind shear mechanism as responsible for temperate latitude E_s. In this model compression of meteoric atomic ions into thin layers is caused by ions converging at nodes in the vertical ion drift profile, brought about by the action of the horizontal wind forcing ions down the geomagnetic field (from above a node) and up the geomagnetic field from below: a situation only possible in the dynamo region where the ion–neutral collision frequency, ν_{in}, exceeds the ion gyro frequency, ω_i. At heights $\leq$120 km, the zonal wind is the main factor (a westward wind above and an eastward wind below the node corresponding to a negative shear) because $\nu_{in} \gg \omega_i$. Conversely at heights $\geq$120 km, the meridional wind is also operative. The shears responsible for E_s are thought to arise from the height profile of both the solar semidiurnal tide (modes 2,2 and 2,4) and internal gravity waves originating in the lower atmosphere. Tidal motion leads to a wind vector which rotates clockwise (in the northern hemisphere) and having a vertical wavelength which increases with height. Because of the phase properties, the overall wind pattern descends so that long-lived meteoric ions trapped in a node where their virtual velocity is zero will descend as the node descends. Ion collection efficiency is low for heights $\leq$100 km because of loss processes and ionisation is dumped into the D-region.

In seeking the governing factors responsible for E_s one approach is to compare observations with the predictions of the wind shear theory. A simple model predicts (Whitehead 1971) that the maximum ionisation density N in an E_s layer should depend on the ambient meteoric ionisation density N_0, the zonal wind shear $\partial U/\partial z$ and H the horizontal component of the geomagnetic field as

$$N \propto N_0 \left(\frac{\partial U}{\partial z}\right)^{\frac{1}{2}} H^{\frac{1}{2}},$$

though Whitehead argued that a stronger H dependence may be more realistic. Since meteoric ions (Fe^+ dominantly) are created by charge exchange from

ambient E-region ions O_2^+ then

$$N_0 \propto (f_0 E)^2 N_m,$$

where N_m is the number density of neutral meteoric atoms: the available reservoir of meteoric species resulting from the ablation of meteoroids. Further, N_m is a function of height and also varies diurnally and seasonally.

Table 1. Stations of the survey

	Geographical		Period	Occurrence (%) $f_0 E_s \geq 5$ MHz daytime			
	lat. S	long. E	data	Summer	Autumn	Winter	Spring
Port Moresby	9°·4	147°·1	1962–70	22·8	9·9	12·2	10·4
Townsville	19·6	146·8	1957–82	33·4	19·1	8·6	7·7
Rarotonga	21·2	200·2	1970–80	23·3	9·6	4·4	12·1
Brisbane	27·5	152·9	1957–85	37·0	13·8	11·9	5·2
Norfolk Is.	29·0	167·9	1964–84	42·3	15·0	9·4	9·9
Mundaring	32·0	116·2	1957–85	28·4	6·9	4·8	1·6
Canberra	35·3	149·0	1964–85	38·9	8·0	8·7	2·0
Hobart	42·9	147·3	1962–83	20·2	2·3	4·7	0·2
Christchurch	43·4	172·4	1970–86	28·9	2·8	10·0	0·7
Campbell Is.	52·6	169·1	1978–85	7·8	6·4	2·1	3·8

2. The Survey

The hourly values of ionosonde E_s parameters were analysed for ten stations in the Australasian South Temperate zone (Table 1). The geographical area covered was about 40°×80° and the data were available for several decades in some cases. In this paper the latitudinal–seasonal characteristics of E_s are studied measuring the occurrence of $f_0 E_s$.

The statistical nature of E_s with large fluctuations in ionosonde frequency parameter values makes it important to choose a parameter that is meaningful in representing changing conditions. Many studies make use of the percentage of samples for which $f_0 E_s$ (or $f_b E_s$) exceeds some limiting value. The choice of this limit is a compromise: too low a value of $f_0 E_s$ yields occurrence probabilities near saturation which therefore produce no useful signature (they will also be contaminated by the normal E-region if $f_0 E_s$ is not greater than noon $f_0 E$); while too high a value will yield a probability so small as to be a poor estimate affected by random fluctuations. For the survey the limiting values of $f_0 E_s \geq 5$ MHz were used.

3. Results

Fig. 1 shows contour displays of the seasonal–diurnal activity for all stations while Fig. 2 presents the seasonal variations for fixed (3 hourly) local times. Examination indicated that the patterns of $f_0 E_s$ activity show no significant dependence on solar cycle. With nearly three decades of data each individual point in Fig. 2 represents up to 600 hourly values so that each pattern of station activity represents long term E_s occurrence free of the effects of significant fluctuations. In Fig. 2 with the ordinate markers representing occurrence probabilities of 20% the uncertainties obtained from year to year fluctuations are about ±0·05 of the ordinate values. In that sense much of the

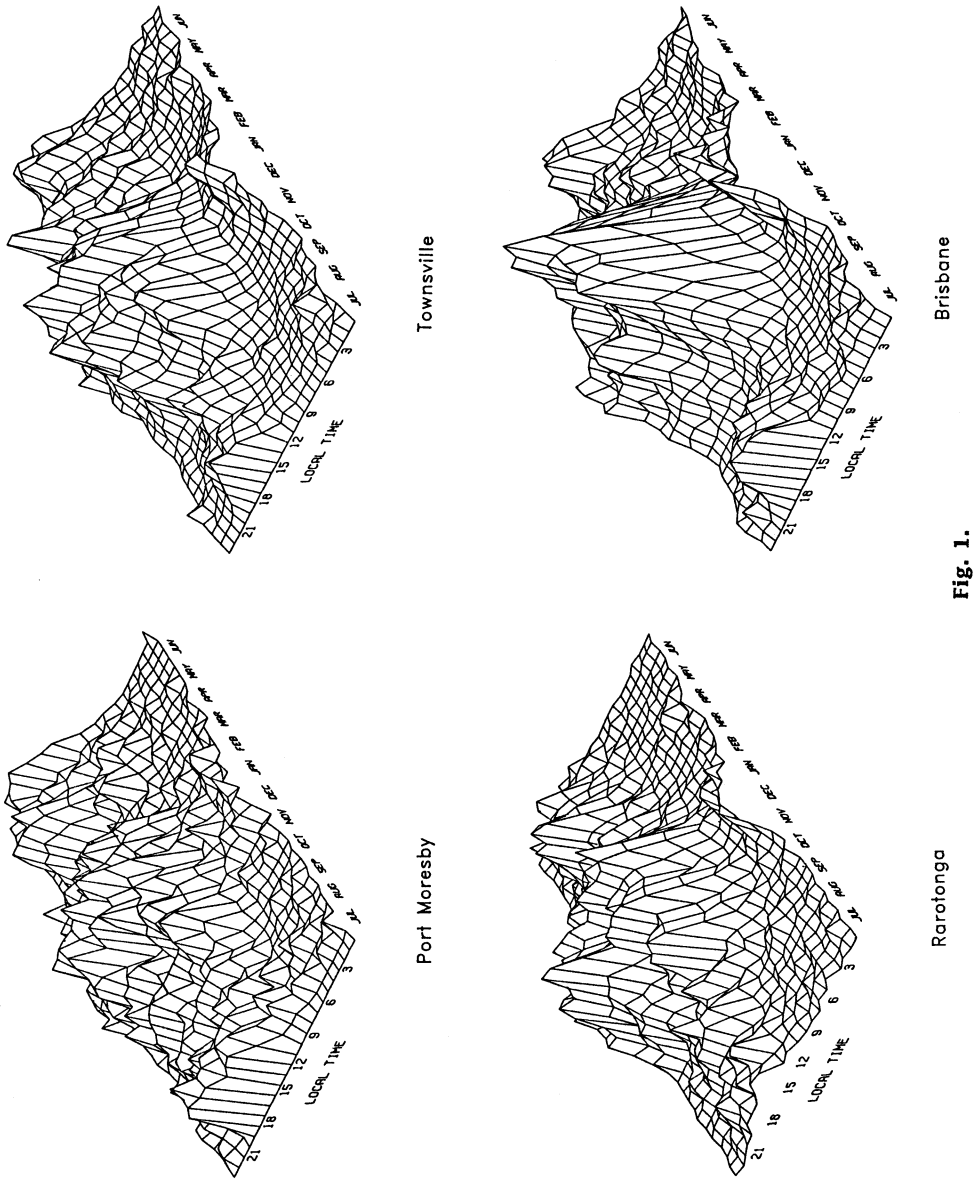
JAN MAR MAY JUL SEP NOV JAN FEB MAR APR JUN AUG SEP OCT NOV DEC JAN
LOCAL TIME
3 6 9 12 15 18 21
Townsville
Brisbane
Port Moresby
Rarotonga

Fig. 1.

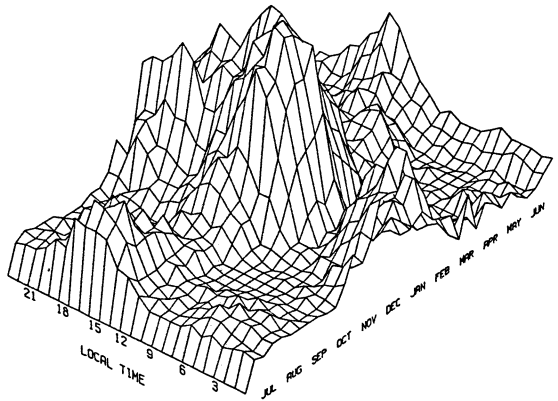

Norfolk Island

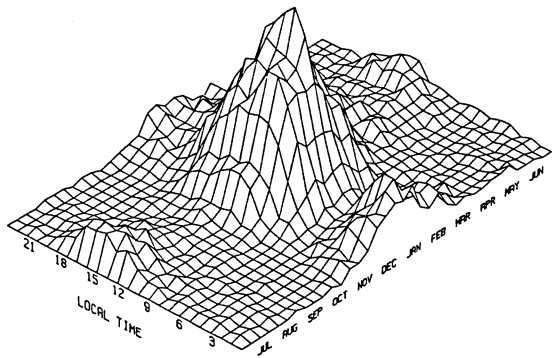

Mundaring

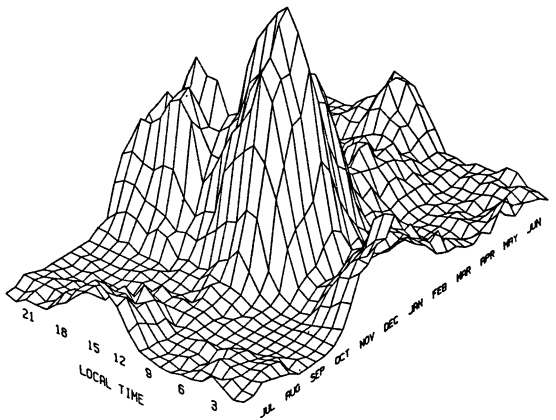

Canberra

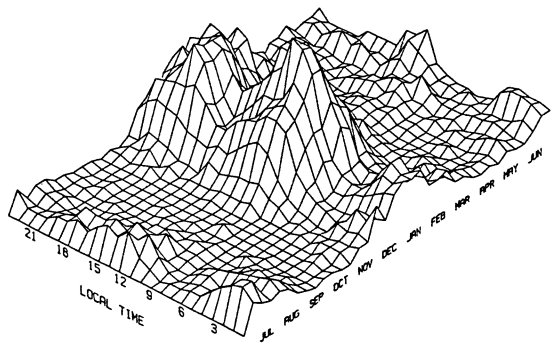

Hobart

Fig. 1. (*Continued*)

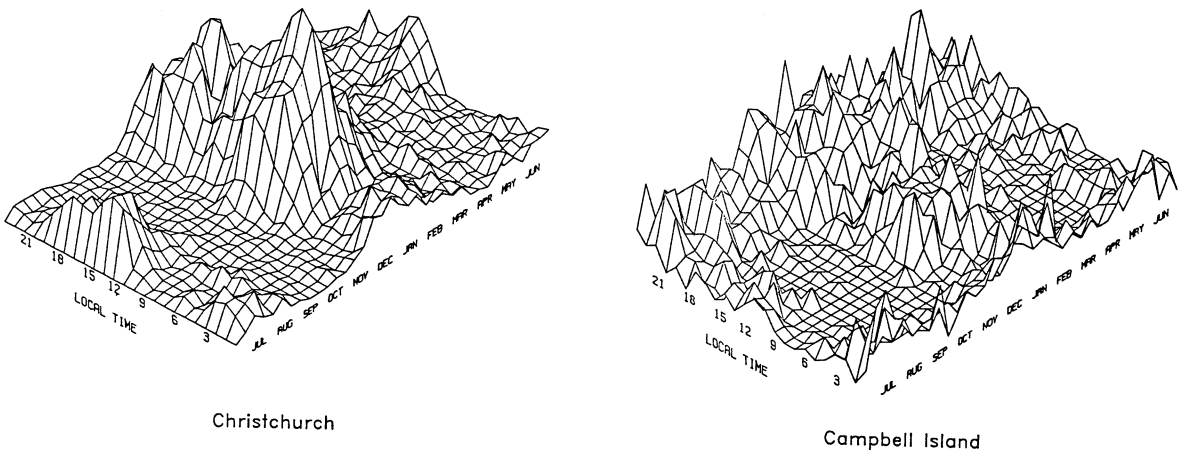

Fig. 1. Seasonal–diurnal characteristics of the average (over ~20 years) occurrence of $f_0 E_s \geq 5$ MHz for the ten stations of the survey. Sampling intervals are 10 days and 1 hour.

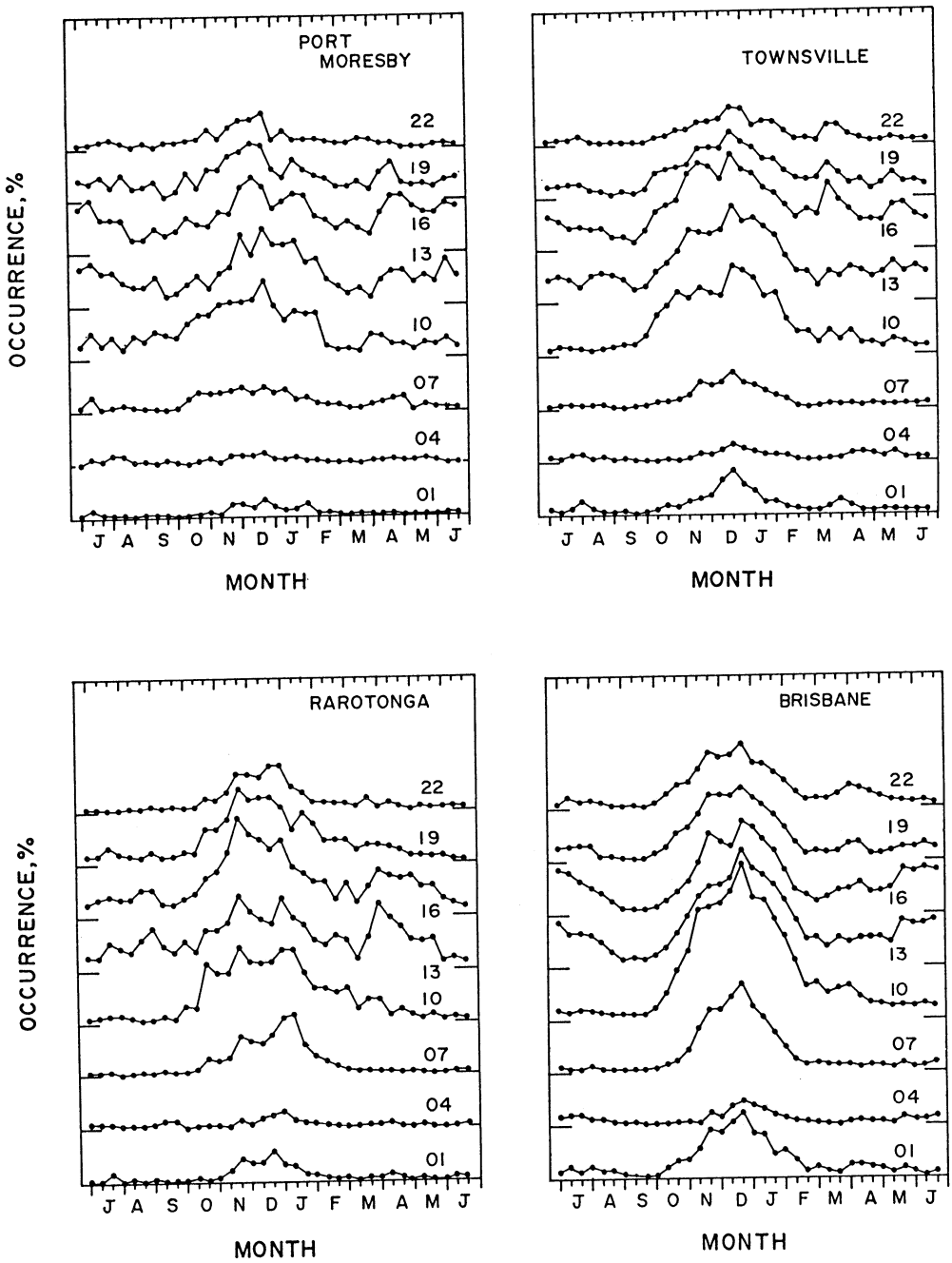
PORT MORESBY
TOWNSVILLE
RAROTONGA
BRISBANE
OCCURRENCE, %
OCCURRENCE, %
22
19
16
13
10
07
04
01
J A S O N D J F M A M J
MONTH
MONTH
MONTH
MONTH

Fig. 2.

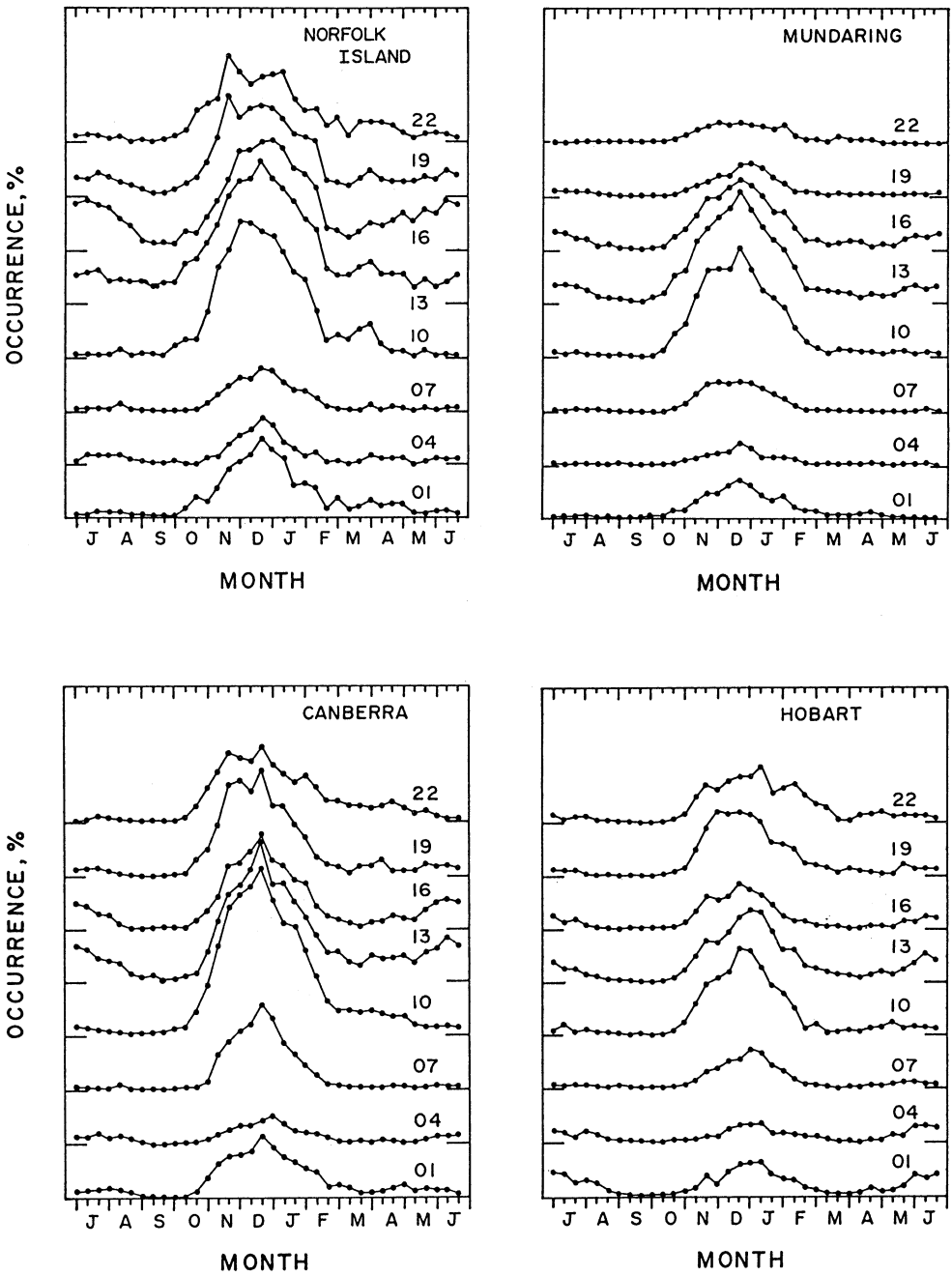

Fig. 2. (*Continued*)

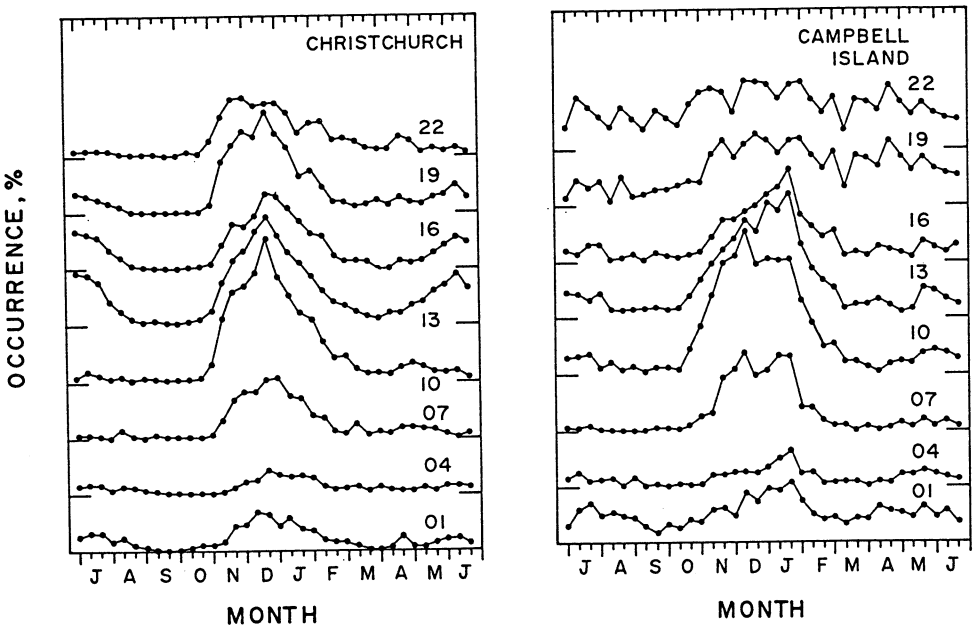

Fig. 2. Seasonal variations of the average occurrence of $f_0 E_S \geq 5$ MHz (for Campbell Island 4 MHz was chosen for illustration due to low occurrence) for the ten stations of the survey. The variations are shown for different local times at 3-hour intervals. The plot labelled 01 is the mean of values at 00, 01 and 02 LMT. The horizontal ticks (separation 20%) on the ordinate are the zero for each plot. Each datum point is evaluated using 20 years (approx.), 10 days, 3 hours yielding 600 hourly values. The uncertainty in each datum point on the plots is about ±0·05 of the datum value

seasonal variations (10 day sampling) depicted in Fig. 2 are realistic effects and not statistical in nature.

There are several gross characteristics: the diurnal summertime activity is dominated by peaks at about 1000 and 1900 LMT at mid-latitudes but by a single broad daytime maximum at low and high latitudes; a winter afternoon 1300–1500 LMT enhancement occurs at all latitudes; well-defined equinox minima occur at most latitudes (with spring less than autumn; in contrast for Campbell Island the evening–midnight period shows little seasonal variation).

In addition to these large-scale (months) variations there are two short-term (several weeks) features. An autumnal enhancement is evident at low latitudes. Referring to Fig. 2, this enhancement is present for Port Moresby April 25 (1600–1900 LMT), Rarotonga April 1 (1300–1600), Townsville March 25 (1600–2200) and Brisbane April 1 (1900–2200). This autumn enhancement is a consistent feature evident every year for Rarotonga and seems to be strongest therefore at latitudes approximately 20°S.

A pre-solstice peak. Many of the seasonal plots (Fig. 2) indicate a minor trough occurring about December 10 and a peak about November 25. This feature is discernible sometimes as a distinct peak or sometimes as a change of slope in afternoon–evening activity for mid-latitudes: Townsville 1000–1900 LMT,

Rarotonga 1000–1900, Norfolk Island 1900–2200, Brisbane 1000–2200, Hobart 1000–1600 and Christchurch 1900–2200.

4. Analysis

In order to compare the observations with a (wind shear) model, it is useful to proceed by examining the seasonal characteristics of $f_0 E_s$ activity. In Table 1, columns 5–8 give the percentage occurrence of $f_0 E_s \geq 5$ MHz for day, defined as 0900–1700 LMT, summer (Jan. and Dec.), winter (June and July), autumn (March minimum) and spring (September minimum).

In order to relate the variations of observed percentage occurrence to changes in the relevant physical property of an E_s layer (i.e. the peak ionisation density N), it is necessary to examine the dependence of occurrence on limiting frequency employed. For the data of the survey limiting frequencies of 3 to 9 MHz were used to form an analytical relation. The data conformed well to the rule

$$\log_e P = a - b(f_0 E_s), \tag{1}$$

where P is the percentage occurrence of ordinary ray frequency data being in excess of a value $f_0 E_s$ with $b \approx 0{\cdot}65 \pm 0{\cdot}1$ (the range of parameter depending on season, and time of day to some extent).

Using the predictions of the wind shear theory,

$$N \propto (f_0 E)^2 N_m \left(\frac{\partial U}{\partial z}\right)^{\frac{1}{2}} H^{\frac{1}{2}}, \tag{2}$$

we can estimate the likely contribution made by each term to the seasonal variations.

Table 2. Latitudinal-seasonal variations of the E_s ionisation N

	$\frac{\cos Z_{aut}}{\cos Z_{win}}$	$\left(\frac{f_0 E_{sum}}{f_0 E_{win}}\right)^2$	$\left(\frac{U_{sum}}{U_{win}}\right)^{\frac{1}{2}}$	N ratio		Observed N ratio	
				$\left(\frac{aut}{spr}\right)$	$\left(\frac{sum}{win}\right)$	$\left(\frac{aut}{spr}\right)$	$\left(\frac{sum}{win}\right)$
Port Moresby	1·15	1·09	1·37	0·72	1·27	0·96	1·45
Townsville	1·36	1·21	1·48	0·85	1·52	1·69	2·10
Rarotonga	1·40	1·22	1·48	0·87	1·53	0·84	2·41
Brisbane	1·58	1·32	1·61	1·00	1·81	1·29	2·25
Norfolk Is.	1·65	1·34	1·80	1·03	2·05	1·75	1·89
Mundaring	1·74	1·39	1·70	1·08	1·88	2·20	2·53
Canberra	1·88	1·46	1·51	1·17	1·87	2·14	2·24
Hobart	2·36	1·66	1·11	1·47	1·56	3·29	2·21
Christchurch	2·39	1·68	1·11	1·50	1·58	2·14	1·83
Campbell Is.	3·63	2·16	1·01	2·26	1·85	1·37	2·06

E-region Ionisation

If we assume a variation of noon f_0E with solar zenith angle χ for Australasian latitudes of the form

$$f_0E \propto (\cos\chi)^{0\cdot3}$$

(see e.g. Beynon and Brown 1959), we get the summer/winter ratio of $(f_0E)^2$ given in Table 2, column 3 for each station.

Meteoric Species

The meteoroid influx to the earth varies due to two principal factors: one is the orbital motion of the earth as it encounters differing populations of dust particles around its orbit, the other is a geometrical effect produced by the tilt of the earth's spin axis. The results of orbit surveys have shown that the background (non-shower) contribution can be simulated as due to radiants close to the ecliptic plane with concentrations at the earth's apex and about ±65° longitude from the apex (see e.g. Davies and Gill 1960). For southern hemisphere stations the apex has its greatest elevation at the autumn equinox and least at the spring equinox. This effect is offset by the larger density of meteoroid radiants encountered by the Earth in the latter half of the year. The resulting influx variation has been measured by Keay and Ellyett (1969). The influx ratios (from their Fig. 5 and accompanying tables) are (Dec.+Jan.)/(June+July) = 0·85; March/Sept. = 1·50.

It is of interest to enquire whether the observed E_s occurrence autumn/spring ratio can be explained in terms of meteoroid influx. This can be assessed by relating the change in ratio with latitude and relating that to the expected latitude variation due to geometrical factors.

At any station the meteoroid influx is greatest near local dawn. At this time in the southern hemisphere the ecliptic has its greatest elevation on March 21 and least on Sept. 23. For a concentration of radiants in the ecliptic, the ratio of influx rates (assumed proportional to cos$Z$ with Z the radiant zenith angle) for each station is shown in Table 2, column 2. [For example a station on the equator would show no difference between autumn and spring since the ecliptic would have the same zenith angle (north in autumn and to the south in spring).] The predicted ratios are based on a simplistic ecliptic radiation distribution but the procedure does demonstrate that the autumn/spring ratio should increase with increasing latitude. Because of the symmetry involved, no difference is to be expected in the summer/winter ratio due to geometrical factors.

Wind Shear

Solar atmospheric tides are excited primarily by the diurnal variations in H_2O insolation absorption in the troposphere and lower stratosphere and O_3 insolation absorption in the mesosphere. In the wind shear model of E_s one would expect that the compressional shear is provided mainly by the regular semidiurnal zonal wind with short-term contributions from erratic gravity wave activity. The vertical structure of the total semidiurnal tides shows significant variation with latitude. The short wavelength modes (2.4), (2.5) are

preferentially damped above 120 km due to increasing molecular dissipation so that the (2.2) mode dominates higher up. In the regime relevant here (100–120 km) the dominant mode is (2.4) with some contribution from (2.2) and (2.5).

For illustration here, the model values given by Forbes and Gillette (1982) (who treated mode mixing) are used and with a simplistic model assuming that the zonal shear ($\partial U/\partial z$) appropriate to any latitude is proportional to the actual peak zonal wind at a height of 110 km. The model predictions of Forbes and Gillette are the same for both equinoxes. Combining the various factors the model (autumn/spring) ratios and the (summer/winter) ratios for the electron density produced by the windshear are shown in columns 5 and 6 respectively of Table 2. Columns 7 and 8 give the observed ratios of plasma densities corresponding to $f_0 E_s$ values as deduced using equation (1).

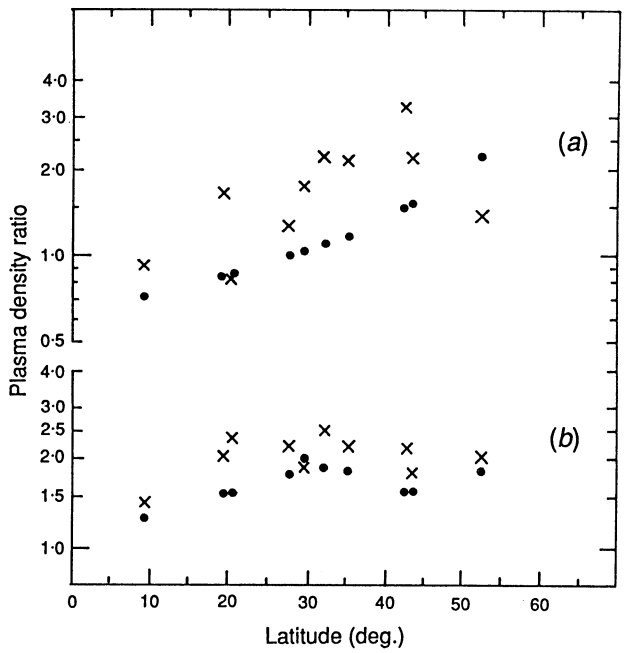

Fig. 3. Behaviour of the E_s plasma densities (deduced from $f_0 E_s$). The ordinate shows the ratios between plasma density values at different seasons as a function of geographic latitude for the ten ionosonde stations. Crosses are observed values and points are the model values: (*a*) Ratios for autumn/spring; (*b*) ratios for summer/winter.

The models and observations are compared in Fig. 3. Although there is some scatter in the data, the general latitude trends of the theoretical and observed values are similar. However, the actual (autumn/spring) model values are generally too low by a factor of about 2.

5. Conclusions

An analysis has been presented of $f_0 E_s$ ionosonde hourly data for ten temperate latitude South Pacific stations over some twenty years to give

averaged seasonal variations. While fluctuations in occurrence are a feature of E_s irregularities, the averages taken over many years will permit the isolation of those seasonal factors controlling E_s production.

The results of this survey can be summarised by three main points:

(i) The gross seasonal variations at all stations except Campbell Island show summer maxima, well-defined equinox minima with autumn greater than spring, and winter afternoon enhancements. A quantitative description has been given that compares the observed ratios (autumn/spring) and (summer/winter) E_s activity with the ratios expected from a wind shear model using known meteoroid influx, background E-region ionisation and semidiurnal tidal characteristics. The latitude trends of the observations and models are not dissimilar though the autumn $f_0 E_s$ activity is consistently greater than predicted from theory.

(ii) A late autumn enhancement in afternoon E_s activity occurs at low temperate latitudes being strongest at about 20°S.

(iii) In the summertime afternoon–evening activity at mid-latitudes there is evidence for a secondary peak one month before the solstice.

No account in the analysis has been taken of the action of internal atmospheric gravity waves in contributing to the shears in the neutral winds as a source of E_s layers. Gravity waves may be generated by any disturbance that causes atmospheric changes on a timescale of minutes to hours. To affect the lower E-region the important sources would be either tropospheric disturbances—weather fronts, depressions, thunderstorms, orthographic perturbations—or local lower thermosphere disturbances such as breaking atmospheric tides. Waves originating in the troposphere increase in amplitude as they propagate up to E-region heights.

Though the dynamics of the lower thermosphere region are characterised by a large spectrum of motions, one simplistic description would be that wind shears due to regular solar tides dictate the long-term characteristics of E_s occurrence, while gravity waves are responsible for the well-known short-term fluctuations in occurrence. Thus, the averages considered in this paper would result in smoothing the effects of day-to-day tropospheric sources.

The seasonal and geographical distribution of gravity wave activity are poorly known. Though data on gravity wave characteristics in the mesosphere are available (mainly from remote radar sensing of plasma dynamics) such work reveals no large Southern Hemisphere seasonal variation (Vincent 1987), only weak maxima at the equinoxes (Vincent 1984).

The late autumn and pre-solstice enhancements of $f_0 E_s$ are small timescale features (~30 and ~10 days respectively) and appear to be annually recurring. The features are not associated with the epochs of any known meteor showers (McKinley 1961; Keay and Ellyett 1969). The question of whether they can be attributed to gravity waves or whether they are a manifestation of solar tidal activity can only be addressed when the morphologies of these phenomena are better understood.

References

Beynon, W. J. G., and Brown, G. M. (1959). *J. Atmos. Terr. Phys.* **14**, 138.
Davies, J. G., and Gill, J. C. (1960). *Mon. Not. R. Astron. Soc.* **121**, 437.

Forbes, J. M., and Gillette, D. F. (1982). A Compendium of Theoretical Atmospheric Tidal Structure. AFGL-TR-82-0173(1).
Keay, C. S. L., and Ellyett, C. D. (1969). *Mem. R. Astron. Soc.* **72**, 185.
McKinley, D. W. R. (1961). 'Meteor Science and Engineering', p. 147 (McGraw–Hill: New York).
Smith, E. K. (1978). *Radio Sci.* **13**, 571.
Vincent, R. A. (1984). *J. Atmos. Terr. Phys.* **46**, 119.
Vincent, R. A. (1987). *Adv. Space Res.* **7**, 163.
Whitehead, J. D. (1970). *Rev. Geophys. Space Phys.* **8**, 65.
Whitehead, J. D. (1971). *J. Geophys. Res.* **76**, 3127.

Manuscript received 6 March, accepted 8 May 1989